# Space-based Bistatic Radar for UAV Autonomous Navigation and Surveillance System

Marc Rodriguez-Cassola*, Michael Oswald†, Marwan Younis*, Luca del Monte‡, Gerhard Krieger*
*Microwaves and Radar Institute, German Aerospace Center (DLR), 82234 Wessling, Germany
†Astrium GmbH Satellites, Military Programs, 88039 Friedrichshafen, Germany
‡European Space Agency, Security Strategy and Partnership Development Office, 75738 Paris, France
Phone/Fax: +498153282392/1449, Email: marc.rodriguez@dlr.de

**Abstract**

Bistatic radars offer several advantages when compared to their monostatic counterparts. In addition to increased performance, sensitivity, coverage and revisit times, all of them parameters which are mainly dependent on their spatial configuration, bistatic radars offer the objective advantage of being more robust to jamming, since the receiver operates as a mere passive system. The proposed system consists of a spaceborne-based radar transmitter illuminating an area of interest and one or several radar receivers mounted on a UAV to perform a two-goal mission: a) help autonomous navigation of the UAV by performing the sense & avoid function, and b) perform surveillance of the overflown area using high-resolution remote sensing techniques. Although the requirements for these significantly different tasks might seem distant, having a spaceborne transmitter ensures that the coverage needed for both purposes is achievable. Assuming the technical feasibility of the complete system, it would provide a cheap and robust manner for enabling global UAV flight, while enabling continuous all-weather imaging capabilities of the UAV-overflown areas with fair resolution values.

## I. Introduction

The feasibility of high-resolution spaceborne-airborne bistatic remote sensing has been recently shown in a series of experiments carried out between the German satellite TerraSAR-X and DLR's new airborne SAR system F-SAR, [1]-[2]. In addition to the different information space measured with the bistatic SAR (as opposed to the monostatic), a significant improvement in terms of SNR and resolution with respect to the spaceborne monostatic system was achieved, mainly because of the shorter ranges receiver-image. Since a SAR is in nature a regular range-Doppler radar, the transmitter signal can also be used to implement a bistatic tracking radar to survey the surroundings of the airplane. Provided that the UAV keeps its nominal track, a task for which real-time scene imaging can be extremely helpful, autonomous navigation can be split into two main tasks: a) sense and track the surrounding flying objects, and b) avoid these flying objects in case the trajectories of the two airplanes collide. Exactly like in the case of a SAR system, the sense and tracking capabilities of the radar can be quantified with measures of range and Doppler resolutions (proportional to speed projection) and the sensitivity of the system [3].

This paper analyses the suitability of a spaceborne-based bistatic radar for allowing both remote sensing and autonomous navigation of a UAV platform. This suitability is discussed in a three-step approach: a) identification and definition of the system requirements, b) general conclusions on the final system, c) proposal of different system examples depending on the desired coverage, and d) performance analysis of the proposed systems. As expected, the presented system shows a moral character with respect to remote sensing and sense and avoid requirements, since persistent coverage opposes to high SNR (close) observations.

## II. System requirements

In defining the system requirements, no a priori condition on the satellite orbit is fixed. Even if some are only academic orbits, any orbit from LEO (200 km) to GEO (35800 km) could be selected. Depending on the selected orbits, the usual trade-off between coverage, repeat cycles and number of satellites can be established. The system requirements definition focus on the UAV characteristics and the required performance of the remote sensing and the sense and avoid subsystems. The fixed characteristics on the UAV flight and dimensions are listed in Table I. The requirements for the remote sensing subsystem are listed in Table II. These values are derived from realistic values of spaceborne and airborne remote sensing systems. The geometrical resolution corresponds to the case of range and Doppler (usually noted azimuth resolution in the

TABLE I
UAV characteristics

| UAV parameter | Range | Typical value |
|---|---|---|
| Velocity [km/h] | [50, 1000] | 130/640 |
| Height [km] | [0.15, 25] | 8/20 |
| Wingspan [m] | [5, 80] | 15/35 |
| Take-off weight [kg] | [500, 10000] | 1000/10000 |

TABLE II

REMOTE SENSING REQUIREMENTS

| **RS parameter** | **Best** | **Typical** | **Worse** |
|---|---|---|---|
| Geometrical resolution [m] | 1 | 5 | 10 |
| NESZ [dB] | $-20$ | $-20$ | $-20$ |
| Revisit times [h] | 0 | 48 | 120 |
| Scene size [km×km] | $2 \times 2$ km$^2$ | $2 \times 2$ km$^2$ | $2 \times 2$ km$^2$ |

TABLE III

SENSE AND AVOID REQUIREMENTS

| **SA parameter** | **Value (worst case)** |
|---|---|
| Range [km] | 27 |
| Bistatic RCS [m$^2$] | 1 |
| Information update period [s] | 1 |
| Information delay [s] | 0.5 |
| Coverage region (height difference) [m] | $\pm 500$ |
| Target velocity range [km/h] | $[0, 1000]$ |
| Reliability [%] | 99.9992 |

SAR case) resolutions. The requirements for the sense and avoid subsystem are listed in Table III. The information update period puts a limit on the integration time of the target. The information delay on the processing time of the radar. The target velocity range has to be doubled, to account for forward and backward-flying objects. The reliability parameter coincides with human reliability and gives information on the constant false alarm rate (CFAR) of the system.

## III. GENERAL ASSUMPTIONS ON THE SYSTEM

On one hand, using a LEO satellite as transmitter improves the overall performance (resolution and sensitivity) of the system, mainly because the transmitter is closer to the scene. On the other hand, sense and avoid function requires persistent monitoring of the area where the UAV is flying, which mixed with LEO condition, results in a constellation with an enormous amount of satellites. If persistent monitoring is desired, MEO-orbit satellite constellations are needed. The previous two conclusions summarise the moral character of the system. Achieving high resolution, high SNR radar images with a MEO constellation guaranteeing constant monitoring in higher frequency bands requires very expensive bandwidths and transmitted powers. Likewise, realistic configurations allowing high resolution and high SNR images [2] cannot guarantee persistent monitoring, and thus are not able to perform the sense and avoid task. Since the MEO solution allows both sense and avoid and remote sensing (with moderate resolutions), whereas the LEO solution only allows remote sensing, we retain as proposed system a MEO constellation guaranteeing persistent coverage of the desired areas.

Sense and avoid range and velocity range conditions fix the first parameter of the system. If classical time-frequency limitation of range-Doppler radars is considered, the carrier frequency has to be strictly under $6$ GHz for unambiguous target localisation. The $\mathrm{PRF}$ is then bounded to a maximal value of $11$ kHz. Since we aim to push the resolution of the system for imaging purposes, the carrier should also be as high as possible. Therefore, C-band is the selected frequency band of the system. Accepting a carrier frequency range between $5$ and $6$ GHz, the $\mathrm{PRF}$ varies between $9.25$ and $11$ kHz. Ideally, the system consists of a C-band MEO satellite constellation illuminating with chirp pulses the interesting areas. These pulses are used for both purposes, and so no further intelligence on the transmitter part needs be included. Ideally too, the receiver is mounted on the UAV and is shared for remote sensing and sense and avoid (the ideally is to be understood as a to be desired. Further analysis on timing and clutter should be performed to ensure the previous statement and therefore this might not be feasible in a final system), and separate antennas are used for remote sensing and sense and avoid. A central unit should in that case be responsible for the time allocation of the receiver to the different subsystems. An integrated positioning unit (usually IMU + GPS) is essential for absolute location of the targets detected by both subsystems.

Receiver remote sensing antennas have to be designed so that image NESZ is better than $-20$ dB, provided that transmitted power, pulse duration and transmitter antenna gain have already been optimized (and fixed) for the satellites. The antennas are side-looking, the only sensible solution for such a system, if acceptable resolution imaging is desired. For imaging a given area, the UAV will flow side-looking to it. Receiver sense and avoid antennas are distributed all around the UAV to guarantee $360^\circ$ surveying of the airplane environment. A scanning on the azimuth plane of the antennas is proposed, and thus the azimuth beamwidth of the antennas is a function of the desired gain and of the properties of such a scanning. The elevation beamwidth depends on the desired gain and on the relative height coverage requirement of the system. Two realistic system examples are presented in the following section. Both solutions use a MEO constellation and have different coverage areas. The first one consists of a reduced Galileo-like ($15$ satellites) constellation allowing persistent global coverage, the second

TABLE IV

REFERENCE SYSTEM PARAMETERS

| | |
|---|---|
| Orbit height [km] | $25000/13300$ |
| Carrier frequency [GHz] | $5.405$ |
| Transmitted bandwidth [MHz] | $100$ |
| Transmitted peak power [kW] | $10/5$ |
| Duty cycle [%] | $20$ |
| Satellite incident angle range [deg] | $[0, 60]$ |
| Antenna size (Tx) | $15$ m parabolic reflector |
| RS antenna size (Rx) | $0.312$ m$^2$ |
| SA antenna size (Rx) | $> 0.0312$ m$^2$ |

one is a lower-orbit MEO constellation (5 satellites) allowing persistent coverage of the polar regions. Both yield remote sensing performance comparable to state-of-the-art radar imaging satellites, showing the advantage of the system. Regarding all the previous considerations, the reference system which will be used for the system examples and performance analysis is presented in Table IV.

## IV. SYSTEM EXAMPLES AND PERFORMANCE ANALYSIS

### *A. MEO constellation for persistent global coverage*

The constellation is a reduced Galileo constellation with three orbital planes and only $5$ satellites per plane, all of them in relative positions of Walker Delta pattern $56°$:$27/3/1$. The orbit height is $25000$ km. Using this configuration, the number of satellites needed for a maximum incident angle of $60°$ is $15$. Figure 1 shows a snapshot of the Earth with the three orbital planes (left) and a snapshot of the density of satellites illuminating the Earth regions (right).

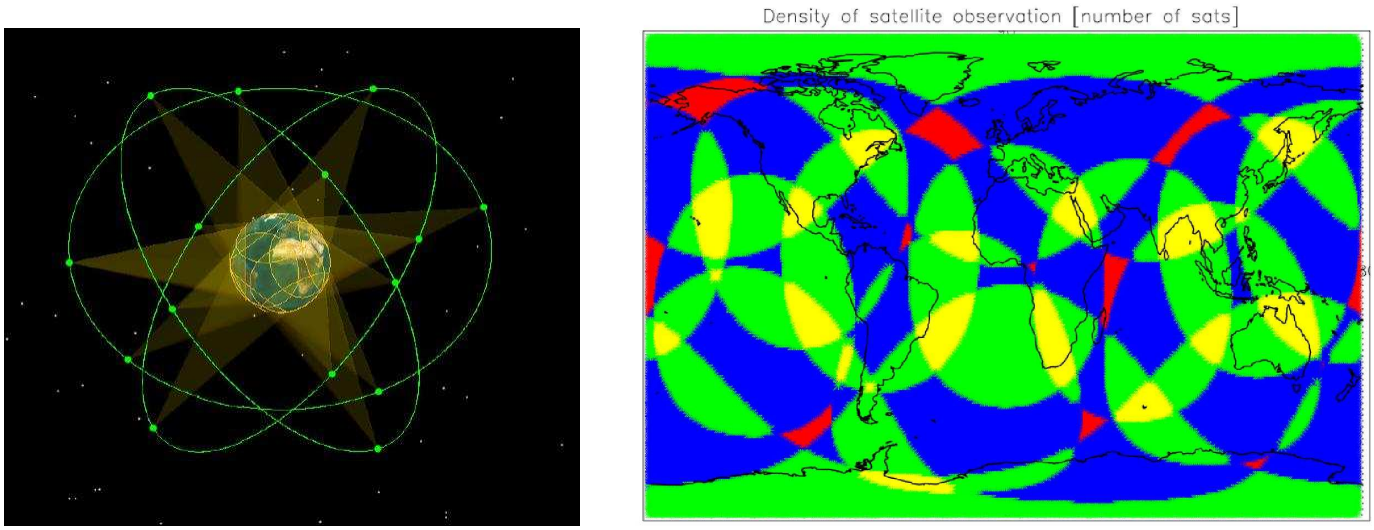


Fig. 1. Snapshots of the 15-satellites MEO configuration for persistent global coverage. Eart plus three orbital planes (left) and density of satellites illuminating the Earth at a given instant: 1 satellite (red), 2 satellites (blue), 3 satellites (green), and 4 satellites (yellow).

*1) Performance analysis of remote sensing subsystem:*

*a) Resolution:* Using the $100$ MHz transmitted bandwidth of the reference system, the range resolution analysis is presented in Fig. 2. In it, we can see the percentage of the Earth which is imaged with a determined range resolution for backward- (left) and forward-scattering (right) cases computed at the mid-beam point of the UAV antenna. The worst resolution in the right plot case has to be understood as the best of the worst, since range resolution may not be bounded for the forward-scattering case. Note that in both cases, the majority of the Earth is imaged with the best possible range resolution. Range resolutions better than $5$ m occur in $99\%$ of the backward-scattering cases and almost $55\%$ of the forward-scattering cases. We remind that range resolution is inversely proportional to transmitted bandwidth [2].

Considering the synthetic resolution (or Doppler resolution, or azimuth resolution, as is usually known in the SAR case), Fig. 3 shows the length of the synthetic aperture required for the C-band system to achieve a synthetic resolution of $5$ m as a function of the UAV height. This length can be directly transformed into required integration time by dividing it by the UAV speed. As expected higher UAV flight heights require longer synthetic apertures. The corresponding integration times

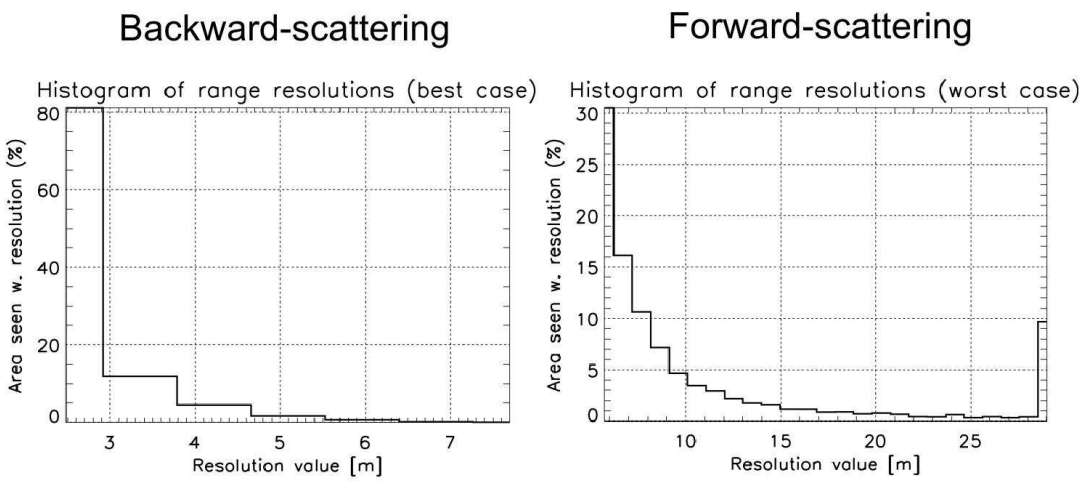


Fig. 2. Percentage of the Earth imaged with corresponding range resolution for backward- (left) and forward-scattering (right) for the 15-satellites MEO constellation for persistent global coverage. The computation is valid for the mid-beam point of the UAV antenna.

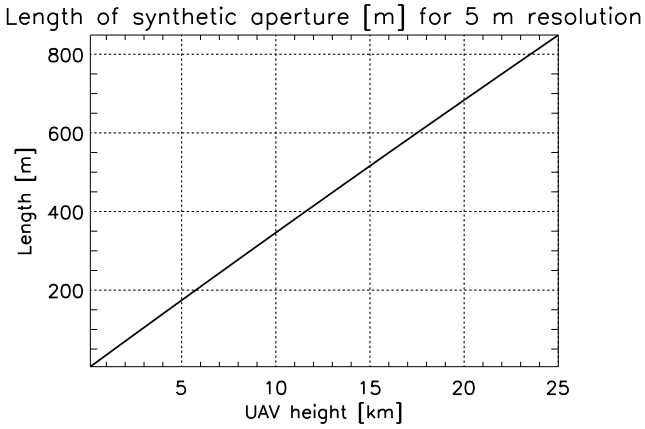


Fig. 3. Length of the synthetic aperture required for achieving a synthetic resolution of $5$ m for the 15-satellites MEO constellation with persistent global coverage as a function of the UAV height.

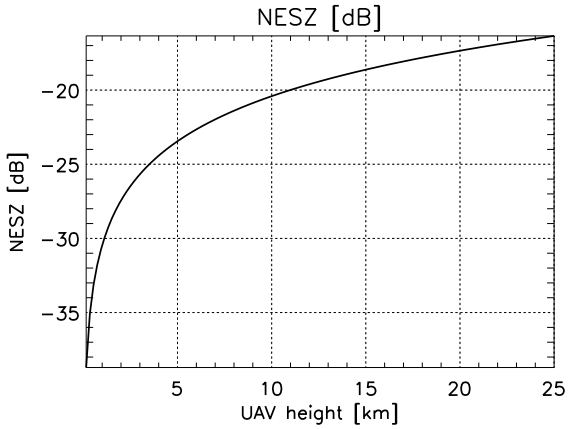


Fig. 4. NESZ for the reference system for the 15-satellites MEO constellation with persistent global coverage as a function of the UAV height.

remain below $8.5$ s for a UAV speed of $100$ m/s, which is within the range of what is currently achievable with state-of-the-art airborne SAR systems.

*b) Sensitivity:* The sensitivity analysis is performed assuming a resolution cell of $5 \times 5$ m$^2$. The transmitted peak power with respect to the reference system is $10$ kW. The NESZ values as a function of UAV height are shown in Fig. 4. We observe that the dependence of NESZ on UAV height is roughly linear, since for all cases the synthetic resolution is kept constant. The NESZ requirement is fulfilled for heights under $11$ km. A transmitted peak power of around $20$ kW would be required for fulfilling the requirement for higher heights.

*2) Performance analysis of sense and avoid subsystem:*

*a) Resolution:* The resolution analysis for the sense and avoid subsystem is rather general and (somewhat) independent of the space constellation considered. Fig. 5 shows the plots corresponding to range (left) and Doppler (right) resolution analysis. The left plot shows the maximum bistatic angle as a function of the transmitted bandwidth and of the desired range resolution. Note that this resolution degrades when targets approach to the baseline vector of the bistatic radar, which is an intrinsic property of bistatic radars themselves. For the $100$ MHz considered case, and assuming a range resolution of $5$ m, the maximum bistatic angle takes a value slightly over $150°$. The right plot on the other hand shows the speed resolution for an extended PRF range and integration times below $0.5$ s. We see that integration times over $0.1$ s already yield resolutions under $1$ m/s, largely sufficient for the foreseen task. This integration time should be tuned after careful analysis of the sensitivity and of the azimuth angle scanning requirements of the system.

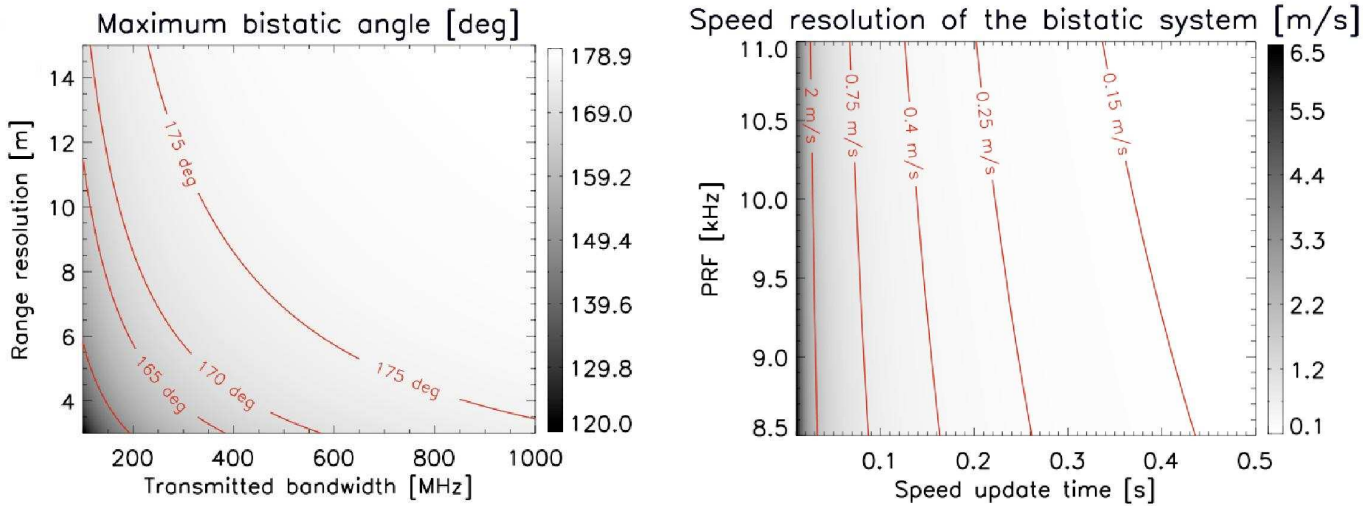


Fig. 5. Range resolution (left) and Doppler resolution (right) analysis for the sense and avoid subsystem. The plots are independent of the space constellation and can be applied to the present and the following subsection.

*b) Sensitivity:* The SNR values after coherent processing of the target echoes (for an integration time of $0.1$ s) and as a function of the satellite off-nadir angle are shown in Fig. 6. Even for the small RCS of the target, its signature is expected to be detected on the radar. Moreover, having an integration time of $0.1$ s allows to achieve an azimuth angular resolution of

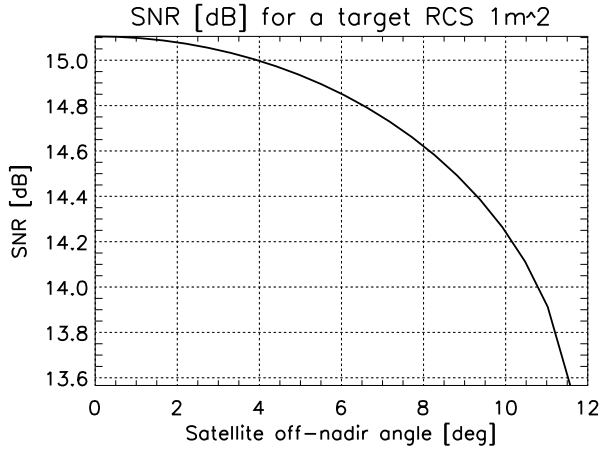


Fig. 6. SNR after coherent integration for a target with a bistatic RCS of 1 $m^2$ for the reference system for the 15-satellites MEO constellation with persistent global coverage as a function of satellite's off-nadir angle and for an integration time of $0.1$ s.

$36°$ using a single receiver.

### *B. MEO constellation for persistent coverage of the polar regions*

The constellation consists of $5$ (for a maximum incident angle of $60°$) satellites in a single orbital plane. The orbit height is $13300$ km, with an inclination of $89.5°$. This orbit height could be affected by the outer Van Allen radiation belt, which might pose problems to the selection of this constellation for a final design. However, since its use does not change significantly the results and conclusions of the study, we retain the example for its illustrative value. We nonetheless remind that a realistic constellation should be placed at a 1000 to 2000 km lower orbit. The deviations in performance would favorise the lower orbits when compared to the ones shown in this case. The proposed constellation guarantees persistent coverage of the polar regions, above $66.55°$ latitudes North and South, respectively. The constellation is particularly advantageous for commanding, since at least one satellite is permanently visible from near-polar ground stations like Kiruna or Svalbard. Figure 7 shows a snapshot of the Earth with the orbital plane (left) and a snapshot of the density of satellites illuminating the Earth regions (right).

*1) Performance analysis of remote sensing subsystem:*

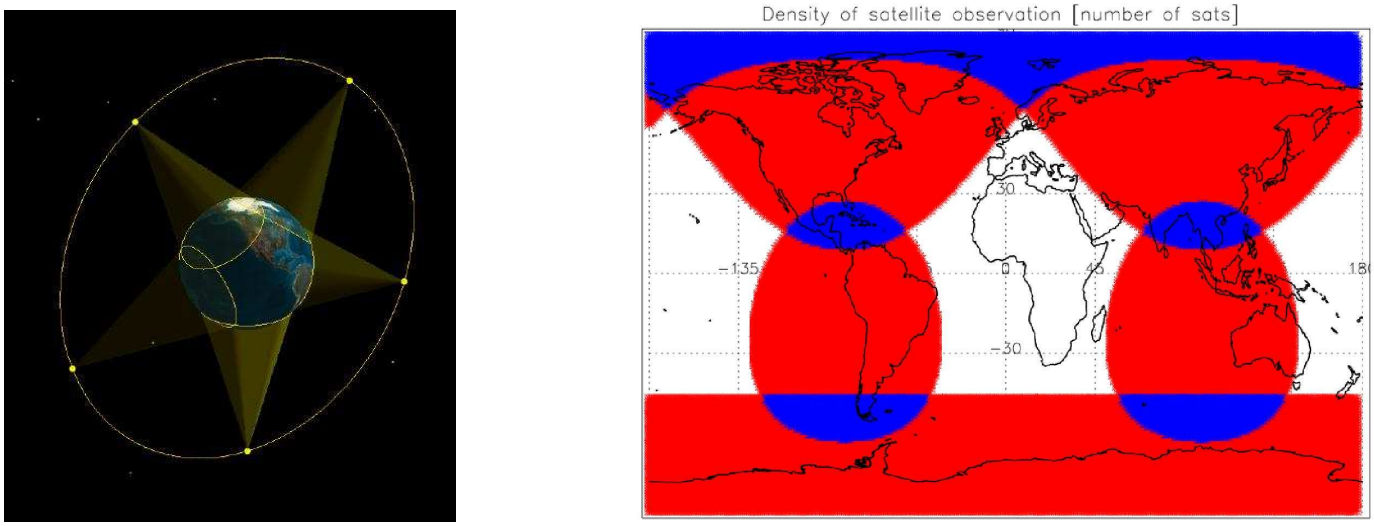


Fig. 7. Snapshots of the 5-satellites MEO configuration for persistent coverage of the polar regions. Earth plus orbital plane (left) and density of satellites illuminating the Earth at a given instant: 0 satellites (white), 1 satellite (red), and 2 satellites (blue).

*a) Resolution:* The same analysis as the one shown in IV-A.1 for the range resolution has been performed. The results are shown in Fig. 8. These resolutions, once again, have been computed for a transmitted bandwidth of 100 MHz and for the mid-beam point of the UAV antenna. Since the incident angle range is exactly the same as the one of the previous constellation and due to the, in general, lesser number of satellites with which a given area is imaged, the flexibility of the constellation to yield a better bistatic configuration (higher incident angles) is lower than for the constellation for global coverage case. Therefore, the results are also a bit worse than those shown in Fig. 2. The tendency is however the same, being the majority of the covered area imaged with the best available range resolution. The synthetic resolution analysis, once again similar to the one

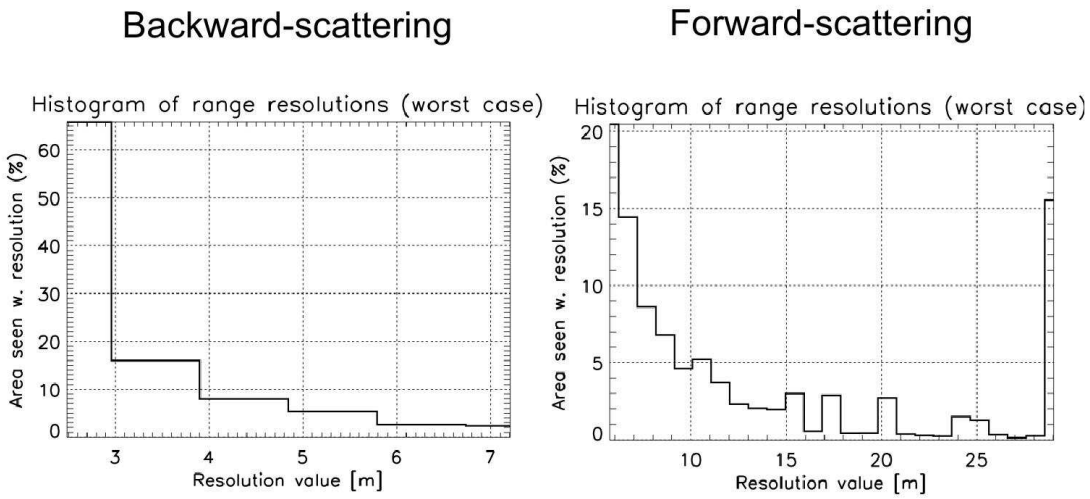


Fig. 8. Percentage of the Earth imaged with corresponding range resolution for backward- (left) and forward-scattering (right) for the 5-satellites MEO constellation for persistent coverage of the polar regions. The computation is valid for the mid-beam point of the UAV antenna.

of IV-A.1, is shown in Fig. 9. The required lengths of the synthetic aperture do not change much, since synthetic resolution is mainly achieved by the motion of the UAV. Like in the case of the global coverage constellation, the corresponding integration times are below of 7.5 s for 25 km UAV flight height. Similar integration times are not uncommon in present airborne SAR systems.

*b) Sensitivity:* The same resolution cell of $5 \times 5$ m$^2$ is used for the sensitivity analysis of this constellation. The transmitted peak power with respect to the reference system is 5 kW. The NESZ values as a function of UAV height are shown in Fig. 10. The dependence of NESZ with UAV height is also linear, like in Fig. 4. The requirement is fulfilled for all almost UAV

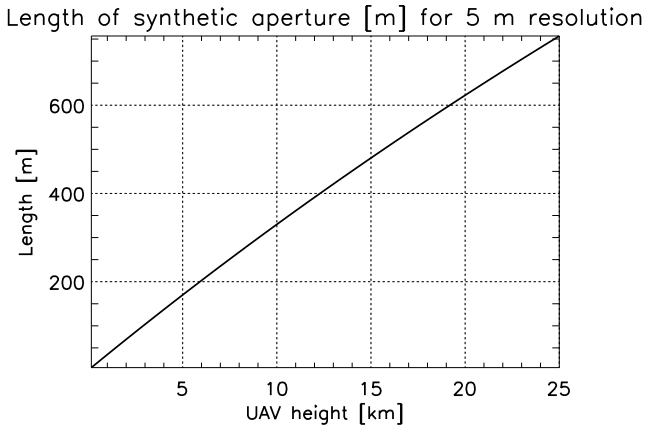


Fig. 9. Length of the synthetic aperture required for achieving a synthetic resolution of 5 m for the 5-satellites MEO constellation with persistent coverage of the polar regions as a function of the UAV height.

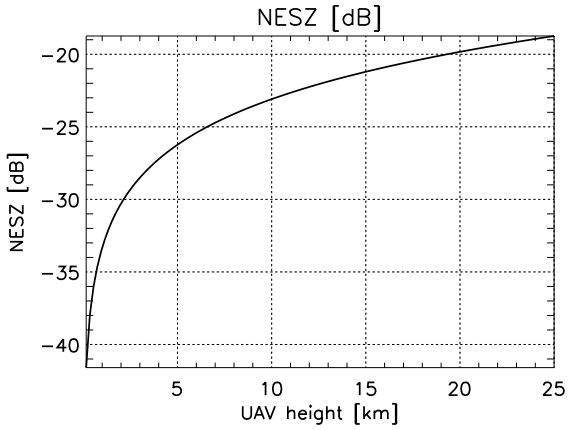


Fig. 10. NESZ for the reference system for the 5-satellites MEO constellation with persistent coverage of the polar regions as a function of the UAV height.

heights. As expected, more reasonable transmitted peak powers are obtained if only partial, though persistent, coverage is required.

*2) Performance analysis of sense and avoid subsystem:*

*a) Sensitivity:* The SNR values after coherent processing of the target echoes (for an integration time of 0.1 s and as a function of the satellite off-nadir angle are shown in Fig. 11. Even for the small RCS of the target, its signature is expected to be detected on the radar. As previously stated, having an integration time of 0.1 s allows to achieve an azimuth angular

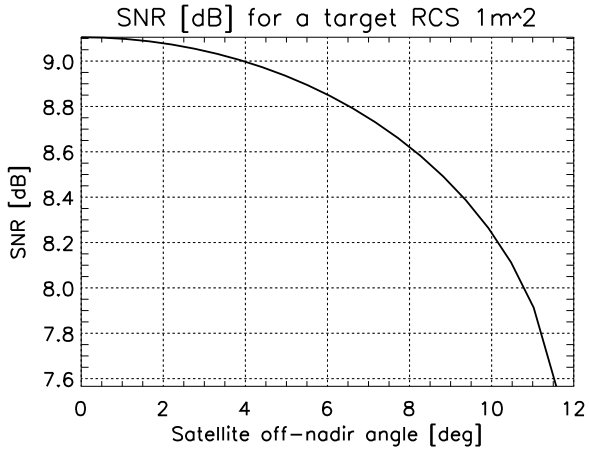


Fig. 11. SNR after coherent integration for a target with a bistatic RCS of 1 $m^2$ for the reference system for the 5-satellites MEO constellation with persistent coverage of the polar regions as a function of satellite's off-nadir angle and for an integration time of 0.1 s.

resolution of 36° using a single receiver.

## V. Summary

A spaceborne-based bistatic radar with a dual character has been presented. The same transmitter is used by two subsystems mounted on a UAV to perform two different tasks: a) high-resolution imaging of interesting overflown areas, and b) help autonomous navigation of the UAV by performing the sense and avoid task on the UAV environment. Some requirements for the system performance and operation have been derived and two exemplary systems with different coverage regions have been designed. The first one allows persistent coverage of the Earht with a 15-satellites Galileo-like constellation. The second one, with 5 satellites placed on a lower orbit, allows persistent coverage of the polar regions. The power and size requirements for the 5-satellites configuration are reduced when compared to the 15-satellites constellation, mainly because of the lower orbit. The performance of both systems in terms of remote sensing are modest if compared to state-of-the-art airborne systems, but competitive (even better) with most of the present spaceborne SAR systems.

## VI. Acknowledgements

This study was funded by ESA Contract no 22448/09/F/MOS.

## References

[1] M. Rodriguez-Cassola, S. V. Baumgartner, A. Nottensteiner, R. Horn, M. Schwerdt, P. Prats, J. Fischer, U. Steinbrecher, R. Metzig, M. Limbach, G. Krieger, A. Moreira, *Bistatic spaceborne-airborne experiment TerraSAR-X/F-SAR: data processing and results*, Proc. IGARSS 2008, Boston, USA.

[2] M. Rodriguez-Cassola, S. V. Baumgartner, G. Krieger, A. Moreira, *Bistatic TerraSAR-X/F-SAR spaceborne-airborne SAR experiment: description, data processing and results*, accepted for publication *IEEE Trans. Geosci. Remote Sens.*

[3] H. Cantalloube, M. Wendler, V. Giroux, P. Dubois-Fernández, G. Krieger, *Challenges in SAR Processing for Airborne Bistatic Acquisitions*, Proc. EUSAR 2004, pp. 577-580, Ulm, Germany.

[4] G. Krieger, M. Younis, *Impact of Oscillator Noise in Bistatic and Multistatic SAR*, IEEE GRSL 3-3, 2006.